Journal of Hydrology 487 (2013) 13–23

Contents lists available at SciVerse ScienceDirect

Journal of Hydrology

journal homepage: www.elsevier.com/locate/jhydrol

Regional-scale variation and distribution patterns of soil saturated hydraulic conductivities in surface and subsurface layers in the loessial soils of China

Yunqiang Wang [a,b,c], Ming'an Shao [b,*], Zhipeng Liu [c], Robert Horton [d]

[a] State Key Laboratory of Loess and Quaternary Geology, Institute of Earth Environment, Chinese Academy of Sciences, Xi'an, Shaanxi 710075, China
[b] Key Laboratory of Ecosystem Network Observation and Modeling, Institute of Geographic Sciences and Natural Resources Research, Chinese Academy of Sciences, Beijing 100101, China
[c] State Key Laboratory of Soil Erosion and Dryland Farming on the Loess Plateau, Institute of Soil and Water Conservation, Chinese Academy of Sciences & Ministry of Water Resources, Yangling 712100, China
[d] Agronomy Department, Iowa State University, Ames, IA 50011, USA

ARTICLE INFO

Article history:
Received 5 December 2012
Received in revised form 3 February 2013
Accepted 7 February 2013
Available online 16 February 2013
This manuscript was handled by Corrado Corradini, Editor-in-Chief

Keywords:
Land use
Soil texture
Principal component analysis
Minimum data set
Geostatistics
Soil hydraulic conductivity

SUMMARY

Saturated hydraulic conductivity (K_s) is an important soil property that shows a high degree of spatial heterogeneity. There is a lack of research that investigates and determines K_s at a regional scale, due to the challenges associated with the required intensive sampling. To determine the closely correlated factors affecting K_s at a regional scale and to then generate a regional distribution map of K_s, we selected 382 sampling sites across the Loess Plateau of China (620,000 km^2) and collected undisturbed and disturbed soil samples from two soil layers (0–5 and 20–25 cm). We found that both surface K_s and subsurface K_s had log(base 10)-normal distributions, and demonstrated strong spatial variability (CV = 206% and 135%, respectively). Surface LogK_s was most closely correlated with LogSand, LogSilt, LogSG (slope gradient), LogSSWC (saturated soil water content), vegetation coverage and land use; while subsurface LogK_s was correlated with LogClay, SSWC, LogSG, LogAltitude, LogGY (growth year) and land use. Geostatistical analysis indicated that semivariograms of surface and subsurface Log K_s could be best fitted by an isotropic exponential model, with effective ranges of 204 km and 428 km, respectively. Distribution maps of K_s produced by kriging indicated a pronounced spatial pattern and demonstrated an obvious spatial depth gradient. The spatial distribution patterns of K_s at a regional scale in the loessial soils of China comprehensively reflected soil hydraulic properties and the combined effects of soil texture, vegetation, topography and human activities.

1. Introduction

Saturated hydraulic conductivity (K_s) is an important soil property that can impact the rates of water and solute transport through soil and influence patterns of infiltration and runoff generation (Buttle and House, 1997; Mallants et al., 1997). In distributed hydrological models, K_s is one of the most sensitive input parameters. However, K_s is characterized by large spatial variability due to the combined effects of physical, chemical and biological processes, which operate with different intensities and at different scales (Santra et al., 2008; Sobieraj et al., 2004). A better understanding of the spatial variation of K_s and of the factors that influence the magnitude and distribution of K_s, as well as their quantitative relationships, is crucial for estimating the flow of water and the transport of solutes across the land-atmosphere boundary and within the vadose zone (Gupta et al., 2006; Russo and Bresler, 1982; Sivapalan and Wood, 1986; Corradini et al., 1998; Morbidelli et al., 2007).

Spatial variation of K_s and its influencing factors may change with increases or decreases in the research scale (scale-dependency). In recent years, the spatial variability of K_s has been studied in different regions around the world (Ciollaro and Romano, 1995; Sobieraj et al., 2004; Zimmermann and Elsenbeer, 2008). Zeleke and Si (2005) studied the spatial variability and scaling of K_s and its soil surrogates along a 384 m transect. They found that several variables demonstrated a certain degree of statistical scale-invariance and long-range dependency; at the observation scale, the variability in K_s was significantly related to sand and silt content, whereas across a wider range of scales, it was related to clay content and soil organic carbon. Buttle and House (1997) investigated the spatial variability of K_s in a 3.22 ha basin and evaluated the effects of macropores on K_s. They found that K_s generally decreased with depth for hillslope podzols and stream valley gleysols. Sobieraj et al. (2002) investigated K_s variation along a tropical

* Corresponding author. Tel./fax: +86 10 64889270.
E-mail address: shaoma@igsnrr.ac.cn (M. Shao).

0022-1694/$ - see front matter © 2013 Elsevier B.V. All rights reserved.
http://dx.doi.org/10.1016/j.jhydrol.2013.02.006

rainforest Kandiudult–Hapludox toposequence and found no relationship between topography and K_s. These studies have increased the understanding of K_s variation at plot, hillslope, and local scales.

However, the majority of past K_s studies have presented data that were obtained at relatively small spatial scales (generally <2 km^2), which were inappropriate for understanding large-scale hydrological processes. With increasing spatial scale, the large-scale factors and processes that govern variation in K_s must be taken into account and the large-scale processes may obscure the contribution of small-scale factors (Gimenez et al., 1999). Therefore, information about large-scale spatial variability of K_s and its related factors is needed to systematically understand large-scale hydrological processes.

Obtaining sufficient and reliable K_s data to determine and characterize the spatial variability of K_s at large-scales (i.e., >100,000 km^2) is challenging due to the high degree of K_s variability and the effort required to collect a sufficient number of soil samples for K_s measurements (Zeleke and Si, 2005). The use of pedotransfer functions (PTFs), which have been derived in various countries in order to estimate K_s indirectly, has been proposed (Buczko and Gerke, 2005; Julià et al., 2004). However, in practice this method has not given accurate results when the PTFs were used outside of the region that they were designed for (Li et al., 2007; Wang et al., 2012a). Therefore, it is important to ground truth the PTFs using direct local measurements of K_s and to adapt them, if necessary.

Soil hydraulic properties are usually influenced by the combined effects of topography, soil, parent material, vegetation, and time (Brantley, 2008). All these factors potentially affect K_s by affecting the soil structure, including the soil porosity and the pore-size distribution. Thus, topography related to the landscape geomorphology affects a series of eco-hydrological processes involving the movement and fate of soil water and soil particles, which can in turn affect soil porosity. Parent material affects the soil texture and mineralogy of the soil particles. Vegetation characteristics (e.g., vegetation coverage, type, and age) affect soil structure by changing the soil physically and chemically, as well as the micro-organism community (Benjamin et al., 2008; Wang et al., 2009). Land use type, which is a human-induced factor, influences the rooting systems and physiology of plants, and soil properties such as bulk density and porosity (Hu et al., 2009). Consequently, all these factors may directly or indirectly, alone or in combination, influence K_s (Zimmermann and Elsenbeer, 2008). However, it is necessary to ascertain or to select the factors that are most closely correlated with K_s from among the large number of potential factors in order to attempt to model and predict K_s effectively.

Previous studies have tended to focus on the variation in the K_s of soil surface layers when the research scale was relatively large. However, due to active soil-forming processes (e.g., eluviation–illuviation between soil horizons) and the impact of human activities on soil structure (e.g. irrigation, tillage and traffic), K_s may vary significantly with soil depth. Factors affecting K_s may also differ spatially at different soil depths and consequently the spatial distribution of K_s itself may also differ with depth (Santra et al., 2008). Hence, characterization of subsurface soils is also important for effective management of water and nutrients in the root zone (Kılıç et al., 2004). It also has important applications for modeling various hydrological processes, such as field-scale infiltration in two-layered soils (Corradini et al., 2011).

Therefore, the objectives of this study were to: (1) characterize the variations in surface and subsurface K_s and related factors across the entire Loess Plateau of China; (2) identify factors that are closely correlated with surface and subsurface K_s using a combination of correlation analysis, principal component analysis, and minimum data set compilation; and (3) generate regional distribution maps of K_s for the two soil layers across the Loess Plateau. Obtaining this information and understanding its applications are useful for assessing hydrological processes at a range of scales (e.g., by downscaling for a deterministic or stochastic framework), and for evaluating the impact of large-scale factors on soil, hydrological and atmospheric processes.

2. Materials and methods

2.1. Description of the study area

The study area was the entire Loess Plateau of China (34–45°5′N, 101–114°33′E) (Fig. 1). The Plateau is in the continental monsoon region, with annual precipitation ranging from 150 mm in the northwest to 800 mm in the southeast; 55–78% of the rain falls from June to September (Shi and Shao, 2000). The annual evaporation is 1400–2000 mm. The mean annual temperature ranges from 3.6 °C in the northwest to 14.3 °C in the southeast (He et al., 2003).

The distribution of soil types was reported by Wang et al. (2011) in detail but, in general, soil textures are coarser in the northwest and finer in the southeast. This distribution pattern of soil texture is closely related to the origin and fallout patterns of the loess deposits in this region. These result from a combination of conditions, which have persisted for 2–3 million years, namely: (1) the rapid uplift of the Tibetan Plateau and surrounding mountain ranges; (2) high rates of sediment production and supply to adjacent basins; (3) a strong northwesterly and westerly wind regime; and (4) the existence of effective dust traps downwind of the source regions (Pye, 1995). Vegetation zones are distributed along a southeast to northwest transect in the general order of: forest, forest-steppe, typical-steppe, desert-steppe, and steppe-desert. The main geomorphic landforms are large flat surfaces with little

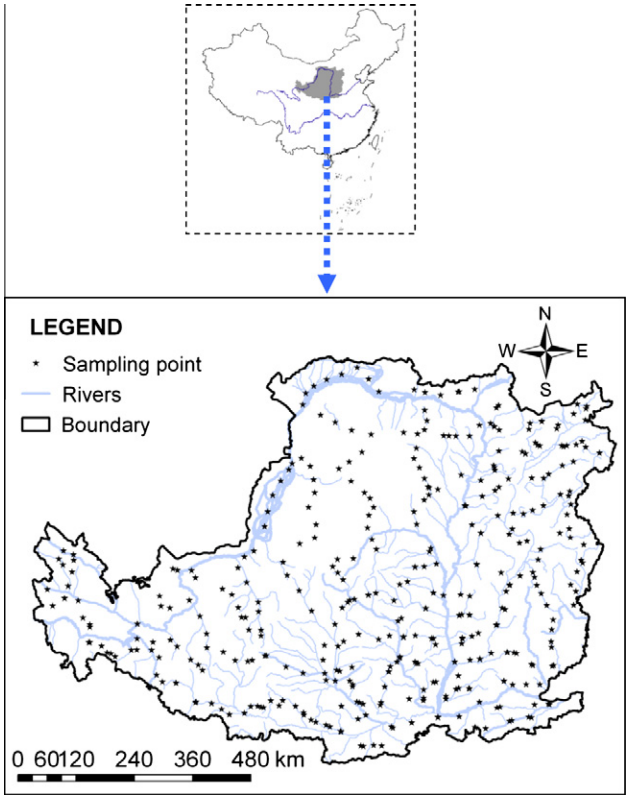

Fig. 1. Location of the Loess Plateau within China and the distribution of the sampling sites.

or no erosion, as well as more erodible ridges and hills, and extensive steep gullies (Shi and Shao, 2000). Fig. 2 illustrates the landforms of the Loess Plateau with the distribution of the vegetation zones.

2.2. Soil sampling and data collection

2.2.1. Soil sampling

To determine accurate values of K_s, we designed an intensive soil sampling scheme that covered the entire Loess Plateau. We chose sampling routes across the Plateau that would use the road transportation system to more conveniently access sites. The spacing between two adjacent routes was approximately 40 km. Sites along the selected sampling routes were also approximately 40 km apart; however, in areas with a more complex landscape and geomorphological type, we decreased the sampling distance to include at least one randomly selected site to better represent the area. In the field, we used a GPS receiver to locate the 382 pre-determined sampling sites (with 5 m precision) (Fig. 1).

The routes that we selected were not confined to paved roads. Many roads were unpaved, earthen roads that had little traffic. Such roads are distributed throughout the Plateau region, even at higher (mountainous or ridge) and lower (gully) altitudes. Therefore, our sampling scheme largely represented the natural geographical conditions of the Loess Plateau.

Sampling sites were selected at least 150 m away from roads to reduce the effects of their presence and use. At each site, undisturbed soil cores were collected in metal cylinders (diameter 5 cm; length 5 cm) to measure K_s, bulk density (BD) and saturated soil water content (SSWC) in the soil surface layer (0–5 cm) and in a subsurface layer (20–25 cm). Disturbed soil samples (about 1 kg) were also collected to determine soil particle composition and soil organic carbon (SOC) contents in the two layers. Over a 6-month period (April to October 2008), we visited 382 pre-selected sites and collected four soil samples at each site: one disturbed and one undisturbed sample taken from each of the two depths. Therefore, a total of 764 undisturbed soil cores and 764 disturbed soil samples were collected.

2.2.2. Laboratory analyses

The K_s of the undisturbed soil cores was determined using the constant head method (Klute and Dirksen, 1986; Wang et al., 2008); BD was determined from the volume–mass relationship for each oven-dried core sample (Wang et al., 2008); SSWC (g H_2O/100 g dry soil) was determined by mass loss from saturated soil samples during oven drying at 105 °C to constant weight, and then it was calculated on a volumetric basis using the determined BD value.

The disturbed soil samples were air-dried and were divided to either pass through a 1 mm mesh or to be crushed to pass through a 0.25 mm mesh. For the samples that passed through the 1 mm mesh, soil particle composition was measured by laser diffraction using a Mastersizer2000 (Malvern Instruments, Malvern, England) (Liu et al., 2005). For the samples that passed through the 0.25 mm mesh, SOC was measured using dichromate oxidation (Nelson and Sommers, 1982). It should be noted that the >1 mm fraction is practically negligible in loess-based soils and this was verifiable by observing that few sand particles were retained on the 1-mm mesh. In addition, the absence of the >1 mm soil particle sizes may reduce scratching of the flow cell walls by quartz grains, for example, that may affect the laser diffraction and the quality of the measurements.

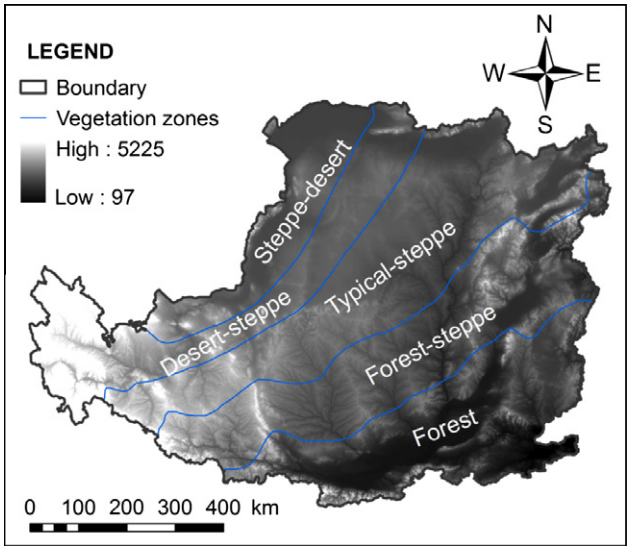

Fig. 2. Elevations of the Loess Plateau and the distribution of vegetation zones.

2.2.3. Environmental conditions at the sampling sites

Altitude, longitude and latitude were determined at each site using a GPS receiver (5 m precision). The information was imported into a geographic information system (Arc/Info) as Albers coordinates. The slope gradient and aspect at each site were measured using a geological compass. Other site-specific parameters that were recorded were land use type (farmland, grassland, forestland), vegetation zone (forest, forest-steppe, typical-steppe, desert-steppe, steppe-desert; see Fig. 2), and vegetation coverage (%). The growth age (years) was ascertained from local people who were familiar with the history of the site land use.

2.3. Data analysis method

2.3.1. Descriptive statistics

Primary statistical parameters including the mean, maximum, minimum, standard deviation (SD) and coefficient of variation (CV) of the measured variables were calculated; these parameters are generally used as indicators of the midpoint and spread of the data. Skewness and Kolmogorov–Smirnov tests were used to determine whether or not the data were normally distributed; non-normally distributed data, including that of K_s, generally needed to be log transformed in order to be normally distributed. Pearson's correlation coefficients were used to determine the strength of possible relationships between K_s and measured soil and environmental factors (Andrews and Carroll, 2001; Lark et al., 2007). Principal component analysis (PCA) was carried out on the variables that were significantly correlated with K_s. The PCA transformed an original set of inter-correlated variables into an equal number of new independent uncorrelated variables or principal components (PCs). The PCs receiving high eigenvalues (>1.0) and comprising variables with a high factor loading (<10% of the highest factor loading) were assumed to be the variables that best explained the variations of K_s (Brejda et al., 2000; Mandal et al., 2008).

After PCA, correlation coefficients and correlation sums were used to reduce redundancy and rule out spurious groupings among the highly weighted variables within a particular PC. These processes reduced the number of variables that were then selected to form a minimum data set (MDS) of variables that best represented K_s. Details of MDS compilation can be found in Mandal et al. (2008) and Wang et al. (2012b).

2.3.2. Geostatistical analysis

Geostatistical analysis was used to produce semivariograms with a best-fit model for K_s that quantified the spatial structure and derived the input parameters for kriging spatial interpolation

(Goovaerts, 1999; Western et al., 2004). The preparation of K_s distribution maps through spatial interpolation of point-based measurements is an important way to display K_s patterns. We used diagnostic plots to explore the spatial data for non-stationarity that may be caused by local trends (Zimmermann and Elsenbeer, 2008).

We derived semivariograms that described the rate of change in K_s as a function of the distance between sampling points using the following equation:

$$\gamma(h) = \frac{1}{2N(h)} \sum_{i=1}^{N(h)} [z(x_i) - z(x_{i+h})]^2 \quad (1)$$

where for each site i, $z(x_i)$ and $z(x_{i+h})$ are values of z at locations x_i and x_{i+h}, respectively; h is the lag and $N(h)$ is the number of pairs of sample points separated by h. Four variogram models (spherical, exponential, linear, and Gaussian) were used to describe the semivariograms, and the best-fitted models, as indicated by the smallest residual sum of squares (RSS) and the largest coefficient of determination (r^2) between model predicted variances and the measured values of K_s, were selected (Wang et al., 2002). Information provided by the best-fitted model was used to analyze the spatial structure of variables.

The semivariogram model describes spatial structure as: $C(h) = C_0 + C_s$. C_0 represents the nugget effect, which is the short-range structure that occurs at distances smaller than the sampling interval, microheterogeneity and experimental error; C_s is the structural component; and $C_0 + C_s$ is the sill (total variance) (Sobieraj et al., 2002). The anisotropy ratio, i.e., the ratio between the slopes of the directions for maximum and minimum variations, was used to identify anisotropy. We considered that there was no significant anisotropy if the anisotropy ratio was less than 2.5, although there is actually no unequivocal index value for identification of anisotropy (Trangmar et al., 1985; Wang et al., 2002).

Spatial distribution maps of K_s at two layers were prepared using semivariogram parameters through ordinary kriging which estimated the value of K_s at unsampled locations by using the following equation:

$$\hat{z}(x_0) = \sum_{i=1}^{n} \lambda_i z(x_i) \quad (2)$$

where $\hat{z}(x_0)$ is the value to be estimated at the location of x_0, $z(x_i)$ is the known value at the sampling site x_i and n is the number of sites within the search neighborhood used for the estimation. The number n was based on the size of the moving window and was defined by the user. The weights, λ_i, depended on the parameters of the semivariogram model and the sampling configuration and were decided under the conditions of unbiasedness and minimized estimation variance. Accuracy of the soil maps was evaluated through a cross-validation approach. Another way of examining the performance of kriging was to calculate the diagnostic statistics of cross-validation. Generally, three statistics: the mean error (ME), the mean squared deviation (MSE), and the mean squared deviation ratio (MSDR) were considered. The model was optimal if these statistics met the following criteria: ME and MSE were close to 0 and MSDR was close to 1 (Webster and Oliver, 2007).

3. Results

3.1. Descriptive statistics

Descriptive statistics, including overall variability and distribution for K_s and the measured soil properties are presented in Table 1. Surface and subsurface K_s values both had high levels of variability, with CV values of 206% and 135%, respectively.

Normality of the data distribution was evaluated using the skewness function and Kolmogorov–Smirnov test. The critical skewness value for the measured 13 variables, having 382 samples from each layer was 0.25 (Tabachnick and Fidell, 1996). The distributions of surface and subsurface K_s values were positively skewed with values of 9.35 and 5.38, respectively (Table 1 and Fig. 3). Values of skewness for most of the measured variables (except for the BD and SSWC of the subsurface layer, and vegetation coverage for both layers) were also greater than 0.25, indicating that the data were non-normally distributed. A logarithmic-transformation (log base 10) was performed on the skewed data before further statistical analyses were conducted. The log-transformed values of K_s were normally distributed (Table 1 and Fig. 3), and the other transformed data were also generally normally or near normally distributed.

Table 1 also shows that the mean values of BD and of the clay and silt contents were lower for the surface layer than for the subsurface layer. In contrast, the mean values for SSWC, SOC, and sand content were larger in the surface layer than in the subsurface layer. The CV values of the BD, SSWC and silt content data, in both the surface and subsurface layers, were relatively low and ranged from 11% to 22%, which indicated that they were relatively uniform. Clay content and SOC data were moderately variable (surface CV: 40% and 70%; subsurface CV: 39% and 67%, respectively). The greater degree of variation in these parameters was likely due to large-scale processes and small-scale fluctuations in the data (Zeleke and Si, 2005).

The environmental factors at the sampling sites located across the entire Loess Plateau, including the topographical parameters of altitude (AL), slope gradient (SG), and slope aspect (SA), and the vegetation traits such as coverage (VC) and growth year (GY), were highly variable across the Loess Plateau (CV values ranged from 43% to 245%) (Table 1). The large ranges of altitude (2879 m), SG (44°), SA (355°), VC (99%) and GY (55 years) may have contributed to the spatial variation of K_s (Hu et al., 2009; Pachepsky et al., 2001).

3.2. Identification and evaluation of factors affecting K_s

3.2.1. Analysis of correlations between K_s and other parameters

We first investigated the impact of two categorical variables (land use and vegetation zones) on K_s at the regional scale. These variables were selected based on expert knowledge. Fig. 4 shows that land use and vegetation zones significantly affected the K_s in both the surface and subsurface layers. The median and mean K_s, for both surface and subsurface layers, increased with land use type in the order: Farmland < Grassland < Forestland (Fig. 4a); in contrast, there were differences in the order of the vegetation zones for K_s in the two soil layers (Fig. 4b). This implied that the mechanisms by which land use and vegetation zones influenced K_s were different. Land use is generally affected and managed by humans while vegetation zones reflect the natural gradients of sunlight hours, temperature and precipitation.

Ordinal categorical variables, such as land use and vegetation zones, were assigned numeric codes, which corresponded to the order of the mean values of K_s. For example, land use in our study was divided into three levels, and the mean values of surface and subsurface K_s for each type of land use followed the order: Farmland < Grassland < Forestland. Thus, land use was represented by three ordinal numerically coded variables: 1 = farmland, 2 = grassland, and 3 = forestland. Similarly, there were five coded numeric values for VZ but these followed two different orders for the two soil layers according to their different affects on the K_s values, namely: 1 = steppe-desert zone (SDZ), 2 = typical-steppe zone (TSZ), 3 = desert-steppe zone (DSZ), 4 = forest zone (FZ), and

Table 1
Descriptive statistics for K_s in two soil layers and other measured soil and site properties (382 observations for each soil layer).

Variables	Depth	Min	Max	Mean	SD	CV	Skewness[a]	DT
K_s	Surface	0.0003	1.87	0.07	0.13	206	9.35	NN
	Subsurface	0.0005	0.79	0.05	0.07	135	5.38	NN
BD	Surface	1.02	1.82	1.34	0.15	11	0.49	NN
	Subsurface	1.03	1.81	1.44	0.16	11	0.05	N
SSWC	Surface	32.8	69.4	50.9	6.0	12	−0.58	NN
	Subsurface	28.8	72.9	47.5	6.1	13	−0.19	N
Clay (%)	Surface	0.44	36	20	7.9	40	−0.45	NN
	Subsurface	0.00	38	21	8.2	39	−0.48	NN
Silt (%)	Surface	6.27	85	69	13	19	−2.62	NN
	Subsurface	7.03	86	69	13	19	−2.63	NN
Sand (%)	Surface	0.81	92	11	17	156	2.97	NN
	Subsurface	0.59	93	9.3	17	181	3.23	NN
SOC	Surface	0.33	40.9	7.6	5.3	70	2.60	NN
	Subsurface	0.29	31.6	5.1	3.4	67	2.56	NN
AL (m)	–	99	2978	1190	517	43	0.74	NN
SG (°)	–	0	44	4	9	224	2.30	NN
SA (°)	–	0	355	42	103	245	2.31	NN
VC (%)	–	1	100	45	33	74	0.14	N
GA (year)	–	1	55	13	14	112	0.98	NN

Notes: K_s, saturated hydraulic conductivity (cm min^{-1}); BD, bulk density (Mg m^{-3}); SSWC, saturated soil water content (cm^3 cm^{-3}); SOC, soil organic carbon (g kg^{-1}); AL, altitude; SG, slope gradient; SA, slope aspect; VC, vegetation coverage; GA, growth age; SD, standard deviation; CV, coefficient of variation (%); DT, distribution type; N, normal distribution; NN, non-normal distribution.

[a] The critical skewness value is $2 \times (6/i)^{0.5} = 2 \times (6/382)^{0.5} = 0.25$; i is the number of observations (Tabachnick and Fidell, 1996).

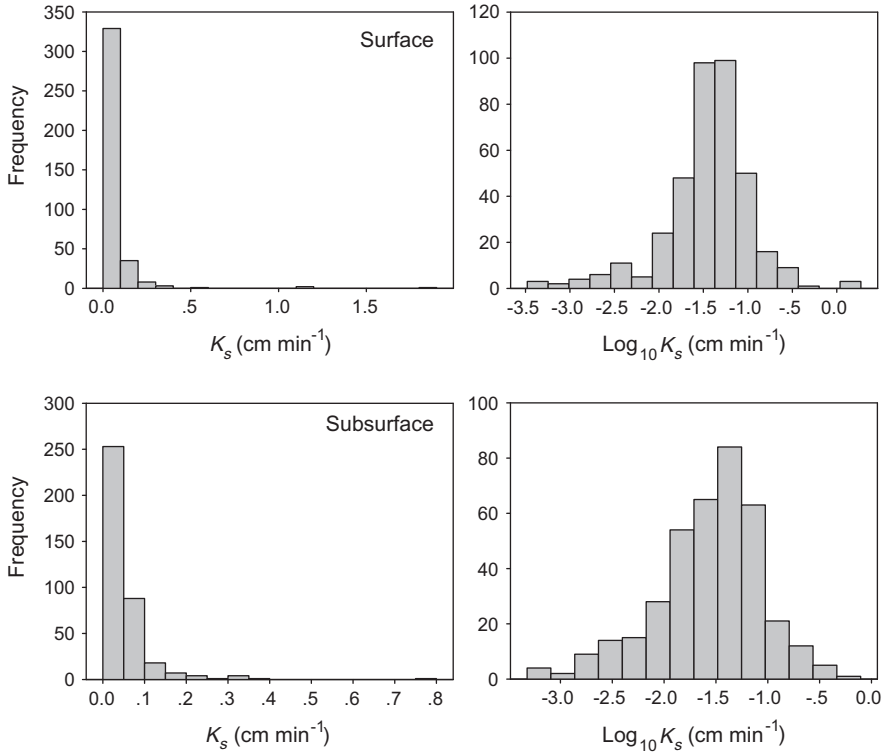

Fig. 3. Histograms of surface and subsurface saturated hydraulic conductivity (K_s) data.

5 = forest-steppe zone (FSZ) for surface K_s; while for subsurface K_s the order was: 1 = SDZ, 2 = FZ, 3 = FSZ, 4 = DSZ, and 5 = TSZ. This procedure enabled correlation analysis, PCA, and regression analysis to be appropriate and meaningful while using ordinal numeric codes for land use and VZ (note: both numeric codes were normally distributed).

The degree of linear association between K_s and the measured soil properties and other related environmental factors (including land use and VZ) on the Loess Plateau were evaluated using Pearson's correlation analysis (Table 2). Surface LogK_s was significantly correlated with 11 of the 13 measured or described variables, i.e., negatively correlated with LogBD, LogSOC, LogClay, and LogSilt ($P < 0.01$) and positively correlated with LogSSWC, LogSand, LogSG, VC, LogGY, land use and VZ, but not correlated with LogAL and LogSA. Subsurface LogK_s showed significant correlations with all of the measured variables ($P < 0.01$). Our observation of the negative

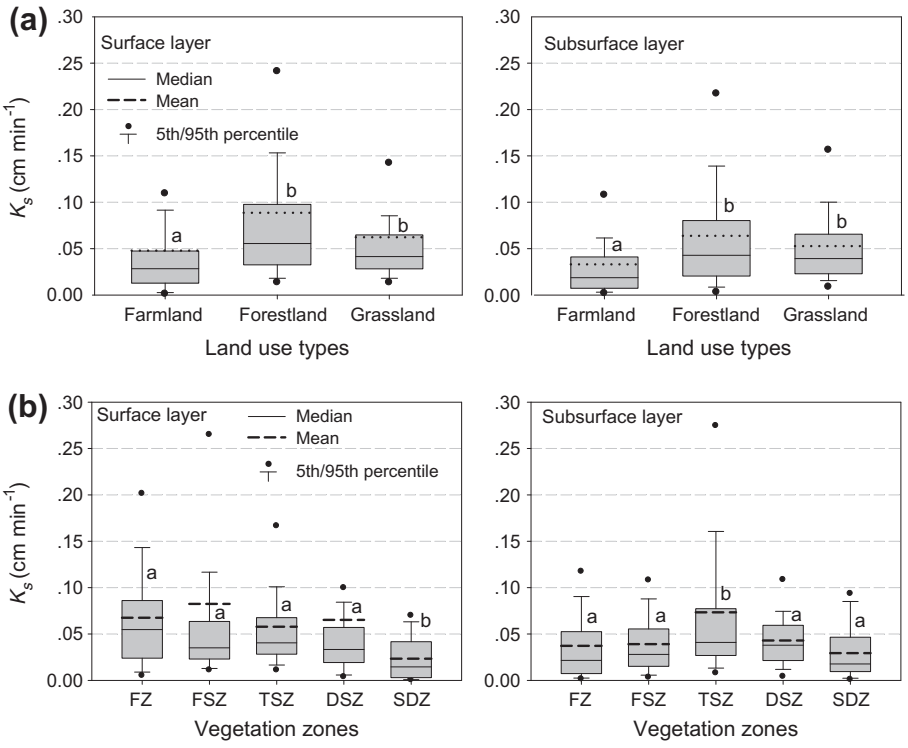

Fig. 4. Effects of land use (farmland, forestland and grassland) and vegetation zone (forest zones, FZ; forest-steppe zones, FSZ; typical-steppe zones, TSZ; desert-steppe zones, DSZ; and steppe-desert zones, SDZ) on surface and subsurface saturated hydraulic conductivity (K_s).

Table 2
Pearson correlation coefficients between saturated hydraulic conductivity (K_s) in surface and subsurface layers, and related factors in the Loess Plateau region; and principle component analysis (PCA) of factors that are most closely correlated with LogK_s (log base 10).

Variables	Pearson correlation coefficient		Surface LogK_s			Subsurface LogK_s			
	Surface LogK_s	Subsurface LogK_s	PC1	PC2	PC3	PC1	PC2	PC3	PC4
BD[a]	−0.36**	−0.41**	−0.677	−0.418	**0.445**	−0.230	**−0.787**	0.147	−0.165
SSWC[a]	0.29**	0.22**	0.654	0.464	**−0.441**	0.164	**0.796**	−0.165	0.142
LogClay	−0.25**	−0.38**	**0.821**	−0.105	0.410	**−0.703**	0.456	0.213	0.168
LogSilt	−0.21**	−0.17**	**0.769**	0.125	0.036	−0.354	0.691	−0.079	0.182
LogSand	0.19**	0.32**	**−0.832**	−0.039	−0.261	0.580	−0.631	−0.215	−0.034
LogSOC	−0.15**	−0.20**	0.644	−0.034	0.254	−0.533	0.361	0.118	0.117
LogAL	*−0.098*	0.22**				0.372	0.115	−0.574	**0.478**
LogSG	0.12*	0.24**	−0.036	0.525	**−0.482**	0.536	0.565	−0.226	**−0.469**
LogSA	*0.10*	0.24**				0.511	0.559	−0.215	**−0.519**
VC	0.23**	0.21**	−0.146	**0.758**	0.375	0.485	0.233	**0.626**	0.190
LogGY	0.34**	0.39**	−0.508	**0.751**	0.152	**0.796**	0.100	0.414	0.148
LD	0.34**	0.30**	−0.296	**0.777**	0.328	0.600	0.128	**0.657**	0.123
VZ	0.15**	0.31**	0.529	0.256	0.107	0.524	−0.170	−0.406	**0.492**
PC analysis	Eigenvalue		3.91	2.50	1.21	3.51	3.22	1.75	1.16
	% of Variance		35.52	22.76	11.00	26.99	24.77	13.44	8.89
	Cumulative %		35.52	58.27	69.27	26.99	51.76	65.20	74.10

Note: Bold type denotes variables with a high factor loading within 10% of the highest loading in a principle component (PC). Numbers written in italics indicate variables mean that were not significantly correlated with LogK_s. BD, bulk density (Mg m^{-3}); SSWC, soil saturated water content (cm^3 cm^{-3}); SOC, soil organic carbon (g kg^{-1}); AL, altitude (m); SG, slope gradient (°); SA, slope aspect (°); VC, vegetation coverage (%); GY, plant growth year (year); LD, land use; VZ, vegetation zone.

[a] For surface LogK_s, the data of surface BD and SSWC were log-transformed (log base 10).

* Correlation is significant at the 0.05 level (2-tailed).

** Correlation is significant at the 0.01 level (2-tailed).

correlation between surface and subsurface LogK_s and LogSOC ($P < 0.01$) was in accordance with the results of Nemes et al. (2005) and Wang et al. (2009). These latter studies also reported similar negative correlations, contrary to the common perception that the opposite would be the case since SOC is usually associated with improved soil structure and hence higher K_s values. Note that a correlation analysis between SOC and other variables is beyond the scope of this study.

The variability in surface and subsurface LogK_s was mainly correlated with soil properties (i.e., soil texture, porosity) and vegetation traits (i.e., vegetation coverage, growth year). The topographic factors (LogAL, LogSG, and LogSA) appeared to play a different role in contributing to the surface and subsurface LogK_s variation, whereby they had weak or non-significant correlations with surface LogK_s (except for LogSG, $P < 0.05$) but significant correlations with subsurface LogK_s ($P < 0.01$).

3.2.2. Principal component analysis

We used PCA to extract the vectors of the correlation matrix for the measured continuous variables of surface and subsurface LogK_s (Webster et al., 1994). The variables that were not significantly correlated with LogK_s were excluded from the respective PCAs because they were weakly related to LogK_s (Table 2).

For the surface LogK_s, the PCA of the 11 correlated variables resulted in three principal components (PC) that had eigenvalues >1 and accounted for 69% of the variance in the data (Table 2). In PC1, LogSand was the greatest contributor to the PC, identified from the factor loadings; LogClay and LogSilt had highly weighted factor loadings (i.e., absolute values within 10% of the LogSand factor loading). PC2 showed that land use was the greatest contributor, followed by VC and LogGY. In the third PC, LogSG was the greatest contributor, followed by SSWC and BD.

For subsurface LogK_s, the PCA identified four PCs that accounted for 74% of the variance (Table 2). The first PC identified LogGY as the best representative variable, followed by LogClay; PC2 was represented by SSWC and BD; PC3 was represented by land use and VC; and PC4 was best represented by LogSA, VZ, LogAL, and LogSG in that order.

The PCA verified the role of soil properties, vegetation traits and topographic factors in explaining surface and subsurface LogK_s variance. A clear impression was gained that surface LogK_s variation was explained in order of importance by soil properties (PC1), land use and vegetation traits (PC2), and topographic factors and soil properties (PC3), while subsurface LogK_s variation was explained in order of importance by vegetation traits (PC1), soil properties (PC2), land use with vegetation traits (PC3), and topographic factors (PC4).

3.2.3. Identification of the most influential variables affecting K_s

Following the PCA, a minimum data set (MDS) of variables intended to predict K_s in each soil layer was created from the variables having a high factor loading in each PC. In a PC that contained at least two variables with a high factor loading, e.g., PC1 (LogSand, LogClay, and LogSilt) for surface LogK_s, we used Pearson's correlation coefficients and correlation sums to further evaluate the correlations and excluded the variable that was most highly correlated with the greatest contributor (details can be found in Wang et al., 2012b). For example, in PC1 for surface LogK_s, LogSand had the highest factor loading (0.832, Table 2) and correlation sum (2.485) and was therefore included in the MDS; then, although LogClay had the second highest correlation sum (2.413), it was excluded from the MDS because it was highly correlated with LogSand ($r = -0.805$, $P < 0.01$); LogSilt had the lowest correlation sum (2.289) but was selected for the MDS, since its correlation with LogSand was less than LogClay's. Hence, two variables (LogSand and LogSilt) were included in the MDS from the PC1 for surface LogK_s.

Using this procedure, variables from PC2 (land use and VC) and PC3 (LogSG and LogSSWC) were also selected and added to the MDS for surface LogK_s. Likewise, variables from PC1 (LogClay and LogGY), PC2 (SSWC), PC3 (land use), and PC4 (LogSG and LogAL) were selected for a separate MDS for estimating subsurface LogK_s. The two final MDSs both included six closely correlated variables for surface LogK_s (LogSand, LogSilt, land use, VC, LogSG and LogSSWC) and for subsurface LogK_s (LogGY, LogClay, SSWC, land use, LogSG, and LogAL). Notably, the MDS was different for the two depths.

3.3. Spatial analysis

3.3.1. Semivariogram

We used geostatistical methods to quantify the specific spatial patterns and structure of LogK_s variation. From the normally distributed dataset of K_s (after log-transformation), we presented the post-plot maps of surface and subsurface LogK_s (Fig. 5). Based on the LogK_s spatial distributions depicted in Fig. 5 combined with Fig. 4, as well as the exploratory data analysis (i.e., trend analysis, Voronoi map), it was concluded that LogK_s did not satisfy the second-order stationarity assumption, especially in the case of the surface layer (Zimmermann and Elsenbeer, 2008). Therefore, we used detrending parameters ranging from zero- to third-order removal to overcome the non-stationarity of the LogK_s data, and then used the detrended LogK_s data to construct semivariograms before determining if there was directional variation based on the anisotropy ratios. Only weak directional variances were detected for LogK_s in the surface and subsurface layers as we found small anisotropy ratios (less than 2.5; Table 3); and thus we calculated omnidirectional semivariograms (Fig. 6) (Wang et al., 2002). We identified the geostatistical model that best fitted each semivariogram from the smallest RSS values and largest r^2 values (Table 3), and we obtained the parameters that provided quantitative expressions of spatial structure.

Table 3 shows that after detrending with third-order removal, the fit of the semivariogram model for surface LogK_s was greatly improved; while for subsurface LogK_s, the improvement was less. Table 3 also listed the semivariogram parameters (range, nugget and sill) for the best-fitted models of surface and subsurface LogK_s and Fig. 6 presents their semivariograms which were best fitted by

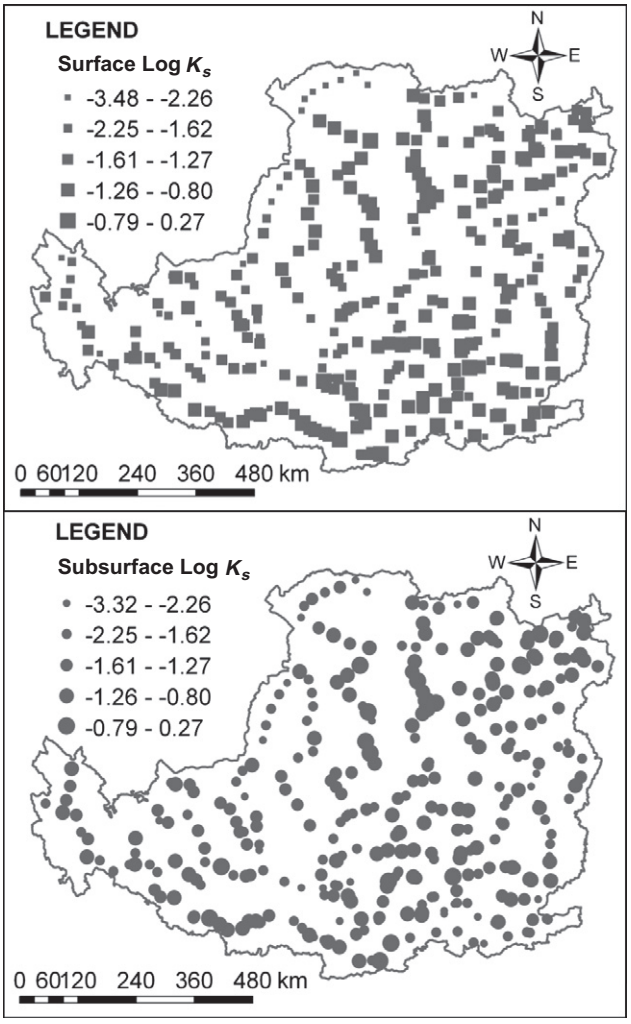

Fig. 5. Post-plot of surface and subsurface LogK_s at the sampling sites on the Loess Plateau.

Table 3
Geostatistical analysis results for LogK_s at surface and subsurface layers (n = 382 for each soil layer). Bold font indicates the parameters of the best fitted semivariogram of LogK_s (K_s unit: cm min^{-1}).

Order of trend removal	Model[a]	Surface layer							Subsurface layer						
		r^2	RSS	Nugget (−)	Sill (−)	Range (km)	ER	AR	r^2	RSS	Nugget (−)	Sill (−)	Range (km)	ER	AR
None	E	0.719	0.00069	0.090	0.220	74	221	1.22	**0.9470**	**0.00035**	**0.120**	**0.260**	**143**	**428**	**1.55**
	L	0.688	0.00078						0.6260	0.00255					
	S	0.619	0.00094						0.7960	0.00139					
	G	0.619	0.00094						0.7970	0.00139					
Constant	E	0.719	0.00070	0.109	0.220	87	262	1.22	0.9450	0.00056	0.129	0.262	156	468	1.55
	L	0.691	0.00078						0.6260	0.00257					
	S	0.621	0.00094						0.7960	0.00140					
	G	0.621	0.00094						0.7980	0.00139					
First	E	0.678	0.00075	0.109	0.219	83	249	1.76	0.9370	0.00048	0.108	0.251	110	331	1.00
	L	0.673	0.00077						0.4600	0.00281					
	S	0.612	0.00091						0.8640	0.00071					
	G	0.612	0.00091						0.8650	0.00070					
Second	E	0.649	0.00078	0.106	0.216	77	231	1.39	0.9450	0.00028	0.116	0.250	118	353	1.15
	L	0.638	0.00081						0.5140	0.00247					
	S	0.589	0.00091						0.8590	0.00072					
	G	0.589	0.00091						0.8600	0.00071					
Third	**E**	**0.727**	**0.00056**	**0.103**	**0.212**	**68**	**204**	**1.77**	0.9160	0.00032	0.058	0.239	69	207	1.14
	L	0.563	0.00073						0.2860	0.00271					
	S	0.644	0.00059						0.8900	0.00042					
	G	0.644	0.00059						0.8910	0.00042					

Note: r^2, coefficient of determination; RSS, residual sum of squares; ER, effective range (km); AR, anisotropy ratio (−).
[a] Model: E, exponential; L, linear; S, spherical; G, Gaussian.

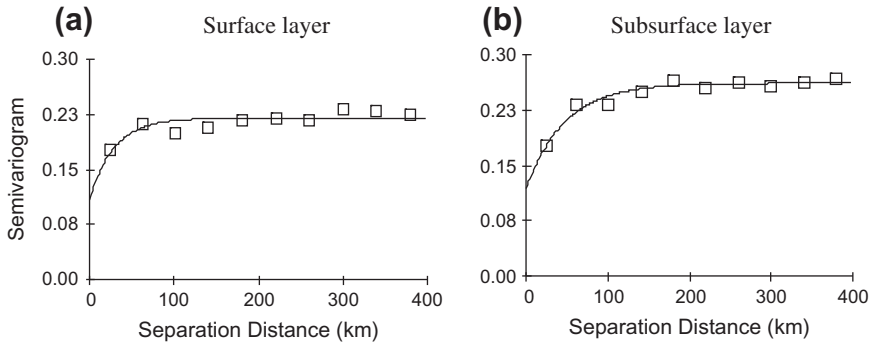

Fig. 6. Semivariograms of K_s for surface (a) and subsurface layers (b) across the entire Loess Plateau in China.

an exponential model. The equation for an exponential semivariogram model is:

$$\gamma(h) = \begin{cases} 0 & h = 0 \\ C_0 + C_s(1 - e^{-\frac{h}{a}}) & h > 0 \end{cases} \quad (3)$$

where h is the lag; C_0 represents the nugget effect; C_s is the structural component; and a is the distance parameter. For surface LogK_s, the nugget variance 0.103 was 49% of the total sill of 0.212. The distance parameter was 68 km, with the effective spatial range of 204 km. The nugget variance of subsurface LogK_s was 0.120 which was 45% of the total sill variance of 0.260. The effective range of subsurface LogK_s (428 km) suggested that there were some larger spatial patterns in the variation than in that of surface LogK_s (204 km).

The value of effective range indicated that the LogK_s values of locations separated with lag distances less than 204 km for the surface layer or 428 km for the subsurface layer were spatially correlated. Beyond these distances, the variation can be defined as random, without significant spatial correlation. Generally, a high proportion of the nugget effect implies a poor model fit to the semivariogram, which would then make the estimated value of the site close to the global average. In the present study, due to the very large studied area, we carried out a high density sampling strategy (n = 382) to generate more reliable semivariograms of surface and subsurface K_s, which can be verified, to some extent, by the value of r^2 and RSS (Table 3).

3.3.2. Spatial distribution of K_s

Producing K_s distribution maps through spatial interpolation of point-based measurements is an important way to display K_s patterns. We used an ordinary kriging interpolation method to produce distribution maps for surface and subsurface LogK_s data across the entire Loess Plateau region. The results were then back transformed to K_s based on the method of Webster and Oliver (2007) (Fig. 7). The same legend was applied to the maps of surface and subsurface K_s so that they could be compared visually. Both maps show spatial patterns of K_s data and, while the two maps are similar in part, there are also some obvious differences.

To test the effectiveness of the models, cross-validation was carried out, and Fig. 8 shows the scatter plots between the actual and predicted values. The results of cross-validation showed the smoothing effect of the spatial prediction. The range of the actual

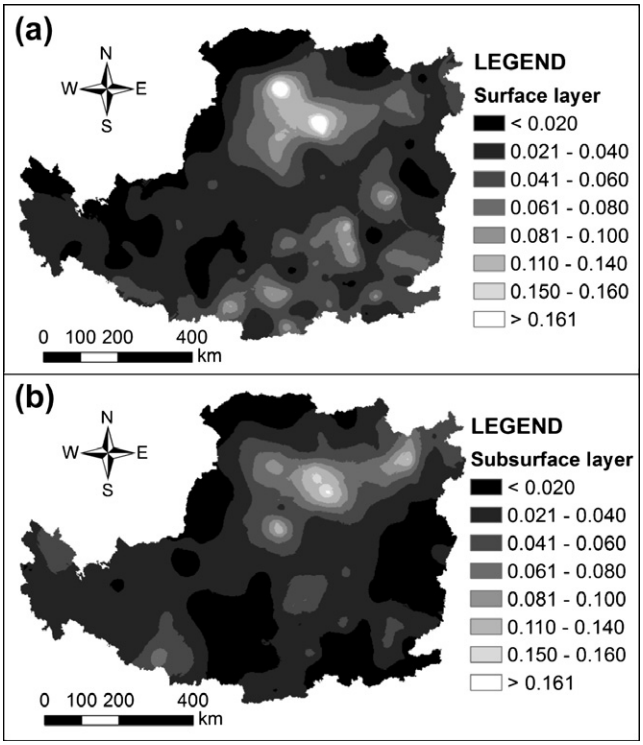

Fig. 7. Spatial distribution maps of surface (a) and subsurface (b) K_s across the entire Loess Plateau region. The interpolation method used was ordinary kriging (unit of K_s: cm min^{-1}).

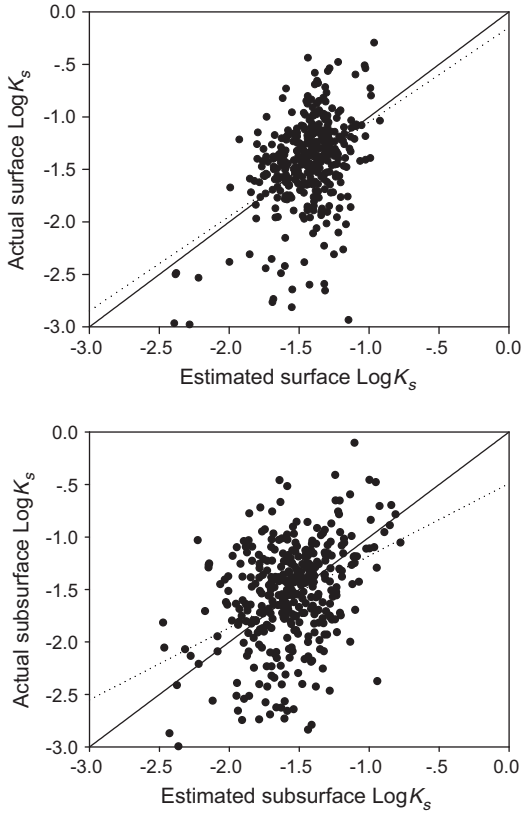

Fig. 8. Cross-validation results showing the differences between the predicted and actual values of surface and subsurface LogK_s. The dotted line is the fitted line and the solid line is the 1:1 line.

Table 4
Performance of ordinary kriging with different orders of trend removal for surface and subsurface K_s (unit: cm min^{-1}) (n = 382 for each soil layer). Bold font indicates the best order of trend removal to be used for the interpolation.

Order of trend removal	ME	MSE	MSDR
Surface layer			
None	0.0039	0.0077	1.050
Constant	0.0039	0.0077	1.050
First	0.0048	0.0096	1.033
Second	0.0038	0.0075	1.028
Third	**0.0031**	**0.0066**	**1.010**
Subsurface layer			
None	**0.0010**	**0.0012**	**0.994**
Constant	0.0011	0.0012	0.993
First	0.0011	0.0013	0.983
Second	0.0018	0.0014	1.018
Third	0.0036	0.0063	1.041

Note: ME, mean error; MSE, the mean squared deviation; MSDR, mean squared deviation ratio.

data for surface LogK_s was −3.48 to −0.27 and that for the estimated data was −2.39 to −0.92. The range for the actual data of subsurface LogK_s was −3.32 to −0.10 and that of the estimated data was −2.47 to −0.78. The smoothing effect of kriging helped to identify the spatial patterns. However, the smoothing effect also indicated that kriging underestimated the larger values and overestimated the smaller ones (Webster and Oliver, 2007). Nevertheless, it should also be noted that the semivariogram models for surface (after detrending) and subsurface LogK_s were acceptable (Table 3), and that the semivariogram-based kriging provided a significantly better estimates than those that would be obtained by using the global mean K_s value of the study area.

In addition, the ME, MSE, and MSDR values for ordinary kriging of surface and subsurface LogK_s with the exponential model were 0.0031 and 0.0010, 0.0066 and 0.0012, 1.010 and 0.994, respectively (Table 4). These statistics were superior to those of spherical, linear, and Gaussian models (data not shown), which indicated a relatively good quality for the kriged maps. Moreover, these statistics further justified the necessity of detrending for surface layer.

The surface K_s values were generally larger than the subsurface K_s values at most of the sampled sites on the Loess Plateau (Table 1 and Fig. 7). In the middle part of the northern Loess Plateau, which is a dry, sandy region, the surface and subsurface K_s were the largest; this region is also known as the Ordos Plateau with sandy soil. Areas with relatively small K_s had a particular spatial distribution (Fig. 7), which generally occurred in the northwestern part around the boundary (Fig. 7a) and in some interior areas such as the southern and eastern parts of the Plateau (see Fig. 7b). The presence of the lower K_s values generally matched the distribution of soil particle composition in the Loess Plateau. A relatively large clay content generally resulted in small K_s values, while a higher sand content favored larger K_s values.

4. Discussion

The magnitude and spatial variation of K_s has been described as a result of several independent processes operating at different spatial scales (Sobieraj et al., 2004; Zeleke and Si, 2005). Processes that are dominant at one scale may not have a significant effect at other scales. Therefore, with increases in scale, local scale processes/factors (i.e., soil structure, biological activity, and tillage) and larger scale processes/factors (i.e., topography, land use, and soil morphology) should be grouped together to evaluate the variation of K_s (Gimenez et al., 1999; Zeleke and Si, 2005). When we studied the variation of K_s across the entire Loess Plateau, we found that both small-scale factors (e.g., soil particle composition, SSWC,

SG, VC, GY) and large-scale factors (e.g., land use type and vegetation zones) significantly contributed to the variation of surface and subsurface K_s (Table 2 and Fig. 4), although the extent of explained variability was different. There have been reports of the significant effects on K_s by small-scale factors, such as soil particle composition (Parasuraman et al., 2007) and bulk density (Bayramin et al., 2009). Here, we pointed out that large-scale factors (i.e., land use type and growth year) should also be considered when evaluating the variability of K_s at larger scales. Mechanisms of land use effects on surface LogK_s can be connected to, for example, tillage and/or management in farmland and grazing in grassland, which may cause differences in soil bulk density, aggregation, and pore size distribution; while the type and growth year of the vegetation may in part indicate the degree of aggregation and macropore formation by roots and macro-biota activity (particularly that of earthworms).

The surface K_s values were generally larger than the subsurface K_s values at most of the sampled sites on the Loess Plateau (Table 1, Fig. 7). Vertical changes in K_s can occur and, in general, it has been reported that K_s decreases with depth (Hu et al., 2009; Mallants et al., 1997; Santra et al., 2008). Our results confirm these findings (Table 1). However, there are some studies where K_s has been found to increase with depth. For example, Zimmermann and Elsenbeer (2008) reported that K_s under pasture increased with soil depth due to the high porosity of weathered sandstones and to steeply inclined stone layers.

The K_s spatial variation was found to be greater for the soil surface than for the subsurface. The strength of the correlations between K_s and BD and between K_s and SSWC also increased with depth (Table 2), which was due to the more complex surface than subsurface processes controlling the K_s variation. The surface soil layer is often disturbed by human activities, for example as a result of fertilization and tillage. These anthropogenic disturbances often alter the natural structure, and increase the porosity and the hydraulic conductivity of the surface soil layer in the short-term. The presence of lower K_s values generally matched the distribution of soil particle composition across the Loess Plateau, in that finer textured soils generally had lower K_s while coarser textures resulted in higher K_s (Santra et al., 2008; Zeleke and Si, 2005). The soil texture distribution pattern is determined by the processes controlling the type and deposition of the windblown particles that comprise the loess in the study area. These processes, whose relative importance varies with the prevailing atmospheric and land surface conditions, include (1) gravitational settling of individual particles; (2) downward turbulent diffusion; (3) advection of dust laden air towards the surface; and (4) wash out of particles by precipitation (Pye, 1995). Subsequently, the deposited loess is often reworked to some degree by the processes of surface wash and soil creep, which enhances the heterogeneity of the soil texture. Ultimately, all of these processes indirectly affect the spatial heterogeneity of hydraulic conductivity both in horizontal and vertical directions.

Finally, it is important to mention that K_s values may vary with time. This has been reported for the Loess Plateau (Hu et al., 2009, 2012) and for other places (Darzi et al., 2008; Logsdon and Jaynes, 1996; Azevedo et al., 1998; Zhou et al., 2008). Various factors such as management practices (Bodner et al., 2008; van Es et al., 1999), rainfall (Gupta et al., 1998; Loague, 1992), drying/wetting processes (Levy et al., 2005; Morbidelli et al., 2011; North and Nobel, 1995), and biological activity (Petersen et al., 2008) have been identified as factors causing temporal changes in K_s. Although significant temporal changes in K_s were found in many places, conflicting results have been reported as to what actually happens with the passage of time; and some studies have even reported that there was no systematic change in K_s spatial variation (Bormann and Klaassen, 2008; Logsdon and Jaynes, 1996). In the present study, due to the time that it took to sample and make measurements at the 382 sites, some temporal effects on K_s may have occurred that were unavoidable. Meanwhile, other variables related to K_s could also be affected by time, e.g., bulk density, vegetation coverage, and SOC. This variation was unavoidable in a study of this scale, and we assumed that the temporal variation of K_s over the 6-month sampling period had a relatively minor influence on the spatial variation of K_s at the regional scale, since soil properties such as particle composition would probably not undergo obvious changes within such a short time.

5. Conclusions

We studied the large-scale spatial variability of K_s in the 0–5 cm and 20–25 cm soil layers across the entire Loess Plateau of China. Surface and subsurface K_s values were log-normally distributed and had relatively large variability ($CV > 100\%$). The overall variability of surface LogK_s (CV = 206%) was greater than the variability of subsurface LogK_s (CV = 135%). Pearson correlation analysis, PCA and MDS compilation identified the closely correlated factors influencing surface LogK_s over large areas, which were LogSand, LogSilt, LogSG, LogSSWC, VC and land use; subsurface LogK_s was strongly associated with LogClay, SSWC, LogSG, LogAL, LogGY and land use. Omnidirectional semivariograms were used to quantitatively characterize the spatial variations of surface and subsurface LogK_s. The effective ranges for surface and subsurface LogK_s values were 204 km and 428 km, respectively. Spatial distribution maps of K_s produced through ordinary kriging indicated clear spatial patterns across the entire Loess Plateau, providing a comprehensive reflection of the soil hydraulic properties under the combined effects of soil texture, parent material, vegetation, topography and human activities (i.e., land use). The magnitudes and spatial patterns of soil hydraulic conductivity in the Loess Plateau demonstrated a pronounced spatial depth gradient.

Acknowledgements

This research was supported by the National Natural Science Foundation of China (Nos. 41101204 and 41071156), the China Postdoctoral Science Foundation funded project (2012T50130), and the State Key Laboratory of Soil Erosion and Dryland Farming on the Loess Plateau (K318009902-1308). Special thanks also go to Mr. David Warrington for his zealous help in improving the manuscript.

References

Andrews, S.S., Carroll, C.R., 2001. Designing a soil quality assessment tool for sustainable agroecosystem management. Ecol. Appl. 11, 1573–1585.
Azevedo, A.S., Kanwar, R.S., Horton, R., 1998. Effect of cultivation on hydraulic properties of an Iowa soil using tension infiltrometers. Soil Sci. 163, 22–29.
Bayramin, I., Basaran, M., Erpul, G., Dolarslan, M., Canga, M.R., 2009. Comparison of soil organic carbon content, hydraulic conductivity, and particle size fractions between a grassland and a nearby black pine plantation of 40 years in two surface depths. Environ. Geol. 56, 1563–1575.
Benjamin, J.G., Mikha, M.A., Vigil, M.R., 2008. Organic carbon effects on soil physical and hydraulic properties in a semiarid climate. Soil Sci. Soc. Am. J. 72, 1357–1362.
Bodner, G., Loiskandl, W., Buchan, G., Kaul, H.P., 2008. Natural and management-induced dynamics of hydraulic conductivity along a cover-cropped field slope. Geoderma 146, 317–325.
Bormann, H., Klaassen, K., 2008. Seasonal and land use dependent variability of soil hydraulic and soil hydrological properties of two Northern German soils. Geoderma 145, 295–302.
Brantley, S.L., 2008. Geology – understanding soil time. Science 321, 1454–1455.
Brejda, J.J., Moorman, T.B., Karlen, D.L., Dao, T.H., 2000. Identification of regional soil quality factors and indicators, I. central and southern high plains. Soil Sci. Soc. Am. J. 64, 2115–2124.
Buczko, U., Gerke, H.H., 2005. Estimating spatial distributions of hydraulic parameters for a two-scale structured heterogeneous lignitic mine soil. J. Hydrol. 312, 109–124.

Buttle, J.M., House, D.A., 1997. Spatial variability of saturated hydraulic conductivity in shallow macroporous soils in a forested basin. J. Hydrol. 203, 127–142.
Ciollaro, G., Romano, N., 1995. Spatial variability of the hydraulic properties of a volcanic soil. Geoderma 65, 263–282.
Corradini, C., Morbidelli, R., Melone, F., 1998. On the interaction between infiltration and Hortonian runoff. J. Hydrol. 204, 52–67.
Corradini, C., Flammini, A., Morbidelli, R., Govindaraju, R.S., 2011. A conceptual model for infiltration in two-layered soils with a more permeable upper layer: from local to field scale. J. Hydrol. 410, 62–72.
Darzi, A., Yari, A., Bagheri, H., Sabe, G., Yari, R., 2008. Study of variation of saturated hydraulic conductivity with time. J. Irrig. Drain. E-ASCE 134, 479–484.
Julià, M.F., Monreal, T.E., Jimenez, A.S.D., Melendez, E.G., 2004. Constructing a saturated hydraulic conductivity map of Spain using pedotransfer functions and spatial prediction. Geoderma 123, 257–277.
Gimenez, D., Rawls, W.J., Lauren, J.G., 1999. Scaling properties of saturated hydraulic conductivity in soil. Geoderma 88, 205–220.
Goovaerts, P., 1999. Geostatistics in soil science, state-of-the-art and perspectives. Geoderma 89, 1–45.
Gupta, R., Rudra, R., Dickinson, T., 1998. Modeling infiltration with varying hydraulic conductivity under simulated rainfall conditions. J. Am. Water Resour. As. 34, 279–287.
Gupta, D.S., Mohanty, B.P., Köhne, J.M., 2006. Soil hydraulic conductivities and their spatial and temporal variations in a vertisol. Soil Sci. Soc. Am. J. 70, 1872–1881.
He, X.B., Li, Z.B., Hao, M.D., Tang, K.L., Zheng, F.L., 2003. Down-scale analysis for water scarcity in response to soil–water conservation on Loess Plateau of China. Agr. Ecosyst. Environ. 94, 355–361.
Hu, W., Shao, M.A., Si, B.C., 2012. Seasonal changes in surface bulk density and saturated hydraulic conductivity of natural landscapes. Eur. J. Soil Sci. 63, 820–830.
Hu, W., Shao, M.A., Wang, Q.J., Fan, J., Horton, R., 2009. Temporal changes of soil hydraulic properties under different land uses. Geoderma 149, 355–366.
Kılıç, K., Özgöz, E., Akbaş, F., 2004. Assessment of spatial variability in penetration resistance as related to some soil physical properties of two fluvents in Turkey. Soil Till. Res. 76, 1–11.
Klute, A., Dirksen, C., 1986. Hydraulic conductivity of saturated soils. In: Klute, A. (Ed.), Methods of Soil Analysis. ASA and SSSA, Madison, Wisconsin, USA, pp. 694–700.
Lark, R.M., Bishop, T.F.A., Webster, R., 2007. Using expert knowledge with control of false discovery rate to select regressors for prediction of soil properties. Geoderma 138, 65–78.
Levy, G.J., Goldstein, D., Mamedov, A.I., 2005. Saturated hydraulic conductivity of semiarid soils, combined effects of salinity, sodicity, and rate of wetting. Soil Sci. Soc. Am. J. 69, 653–662.
Li, Y., Chen, D., White, R.E., Zhu, A., Zhang, J., 2007. Estimating soil hydraulic properties of Fengqiu County soils in the North China Plain using pedo-transfer functions. Geoderma 138, 261–271.
Liu, Y., Tong, J., Li, X., 2005. Analysing the silt particles with the Malvern Mastersizer 2000. Water Conserve. Sci. Tech. Econ. 11, 329–331 (in Chinese with English abstract).
Loague, K., 1992. Using soil texture to estimate saturated hydraulic conductivity and the impact on rainfall-runoff simulations. Water Resour. Bull. 28, 687–693.
Logsdon, S.D., Jaynes, D.B., 1996. Spatial variability of hydraulic conductivity in a cultivated field at different times. Soil Sci. Soc. Am. J. 60, 703–709.
Mallants, D., Mohanty, B.P., Vervoort, A., Feyen, J., 1997. Spatial analysis of saturated hydraulic conductivity in a soil with macropores. Soil Technol. 10, 115–131.
Mandal, U.K., Warrington, D.N., Bhardwaj, A.K., Bar-Tal, A., Kautsky, L., Minz, D., Levy, G.J., 2008. Evaluating impact of irrigation water quality on a calcareous clay soil using principal component analysis. Geoderma 144, 189–197.
Morbidelli, R., Corradini, C., Govindaraju, R.S., 2007. A simplified model for estimating field-scale surface runoff hydrographs. Hydrol. Process. 21, 1772–1779.
Morbidelli, R., Corradini, C., Saltalippi, C., Flammini, A., Rossi, E., 2011. Infiltration-soil moisture redistribution under natural conditions: experimental evidence as a guideline for realizing simulation models. Hydrol. Earth Syst. Sc. 15, 2937–2945.
Nelson, D.W., Sommers, L.E., 1982. Total carbon, organic carbon and organic matter. In: Nelson, D.W., Sommers, L.E., Page, A.L., Miller, R.H., Keeney, D.R. (Eds.), Methods of Soil Analysis, . second ed., Part 2: Agronomy Monograph 9 second ed. ASA and SSSA, Madison, WI, pp. 534–580.
Nemes, A., Rawls, W.J., Pachepsky, Ya.A., 2005. Influence of organic matter on the estimation of saturated hydraulic conductivity. Soil Sci. Soc. Am. J. 69, 1330–1337.
North, G.B., Nobel, P.S., 1995. Hydraulic conductivity of concentric root tissues of agave *deserti engelm* under wet and drying conditions. New Phytol. 130, 47–57.
Pachepsky, Ya.A., Timlin, D.J., Rawls, W.J., 2001. Soil water retention as related to topographic variables. Soil Sci. Soc. Am. J. 65, 1787–1795.
Parasuraman, K., Elshorbagy, A., Si, B.C., 2007. Estimating saturated hydraulic conductivity using genetic programming. Soil Sci. Soc. Am. J. 71, 1676–1684.
Petersen, C.T., Trautner, A., Hansen, S., 2008. Spatio-temporal variation of anisotropy of saturated hydraulic conductivity in a tilled sandy loam soil. Soil Till. Res. 100, 108–113.
Pye, K., 1995. The nature, origin and accumulation of loess. Quat. Sci. Rev. 14 (7–8), 653–667.
Russo, D., Bresler, E., 1982. A univariate versus a multivariate parameter distribution in a stochastic-conceptual analysis of unsaturated flow. Water Resour. Res. 18 (3), 483–488.
Santra, P., Chopra, U.K., Chakraborty, D., 2008. Spatial variability of soil properties and its application in predicting surface map of hydraulic parameters in an agricultural farm. Curr. Sci. 95, 937–945.
Shi, H., Shao, M.A., 2000. Soil and water loss from the Loess Plateau in China. J. Arid Environ. 45, 9–20.
Sivapalan, M., Wood, E.F., 1986. Spatial heterogeneity and scale in the infiltration response of catchments. In: Gupta, V.K., Rodríguez-Iturbe, I., Wood, E.F. (Eds.), Scale Problems in Hydrology. Water Science and Technology Library, D. Reidel Publishing Company, Dordrecht, Holland, pp. 81–106.
Sobieraj, J.A., Elsenbeer, H., Coelho, R.M., Newton, B., 2002. Spatial variability of soil hydraulic conductivity along a tropical rainforest catena. Geoderma 108, 79–90.
Sobieraj, J.A., Elsenbeer, H., Cameron, G., 2004. Scale dependency in spatial patterns of saturated hydraulic conductivity. Catena 55, 49–77.
Tabachnick, B.G., Fidell, L.S. (Eds.), 1996. Using Multivariate Statistics, third ed. Harper Collins, New York.
Trangmar, B.B., Yost, R.S., Uehara, G., 1985. Application of geostatistics to spatial studies of soil properties. Adv. Agron. 38, 45–94.
van Es, H.M., Ogden, C.B., Hill, R.L., Schindelbeck, R.R., Tsegaye, T., 1999. Integrated assessment of space, time, and management-related variability of soil hydraulic properties. Soil Sci. Soc. Am. J. 63, 1599–1608.
Wang, H.Q., Hall, C.A.S., Cornell, J.D., Hall, M.H.P., 2002. Spatial dependence and the relationship of soil organic carbon and soil moisture in the Luquillo, Experimental Forest, Puerto Rico. Landscape Ecol. 17, 671–684.
Wang, L., Wang, Q.J., Wei, S.P., Shao, M.A., Li, Y., 2008. Soil desiccation for Loess soils on natural and regrown areas. Forest Ecol. Manag. 255, 2467–2477.
Wang, T., Wedin, D., Zlotnik, V.A., 2009. Field evidence of a negative correlation between saturated hydraulic conductivity and soil carbon in a sandy soil. Water Resour. Res. 45, W07503. http://dx.doi.org/10.1029/2008WR006865.
Wang, Y.Q., Shao, M.A., Liu, Z.P., 2012a. Pedotransfer functions for predicting soil hydraulic properties of the Chinese Loess Plateau. Soil Sci. 177 (7), 424–432.
Wang, Y.Q., Shao, M.A., Liu, Z.P., Warrington, D.N., 2012b. Investigation of factors controlling the regional scale distribution of dried soil layers under forestland on the Loess Plateau, China. Surv. Geophys. 33, 311–330.
Wang, Y.Q., Shao, M.A., Zhu, Y.J., Liu, Z.P., 2011. Impacts of land use and plant characteristics on dried soil layers in different climatic regions on the Loess Plateau of China. Agr. Forest Meteorol. 151, 437–448.
Webster, R., Atteia, O., Dubois, J.P., 1994. Coregionalization of trace-metals in the soil in the Swiss Jura. Eur. J. Soil Sci. 45 (2), 205–218.
Webster, R., Oliver, M.A., 2007. Geostatistics for Environmental Scientists, second ed. John Wiley & Sons, Ltd., UK.
Western, A.W., Zhou, S.L., Grayson, R.B., McMahon, T.A., Bloschl, G., Wilson, D.J., 2004. Spatial correlation of soil moisture in small catchments and its relationship to dominant spatial hydrological processes. J. Hydrol. 286, 113–134.
Zeleke, T.B., Si, B.C., 2005. Scaling relationships between saturated hydraulic conductivity and soil physical properties. Soil Sci. Soc. Am. J. 69, 1691–1702.
Zhou, X., Lin, H.S., White, E.A., 2008. Surface soil hydraulic properties in four soil series under different land uses and their temporal changes. Catena 73, 180–188.
Zimmermann, B., Elsenbeer, H., 2008. Spatial and temporal variability of soil saturated hydraulic conductivity in gradients of disturbance. J. Hydrol. 361, 78–95.